Problem Chosen	2022	Team Control Number
MCM Problem A	MCM/ICM Summary Sheet	2226471

We recast the problem of finding the optimal power distribution over a cycling race as a nonlinear, constrained optimal control problem and implement a sequential quadratic programming method to generate numerical solutions. To generalize the model to arbitrary courses, we propose a method of optimizing cycling power output over subsections of tracks, called course elements, that may be concatenated into complex tracks.

Under the right boundary conditions between elements, our model's output for complex courses was found to generally agree with the concatenation of solutions to the elements modeling that course. Corroboration with other models supports the viability of SQP for cycling optimization applications for specific ranges of cyclist bioenergetic parameters on tracks without abrupt inclination changes. The optimal power outputs were primarily reflective of course grade, but also responded to certain curvature and wind conditions, indicating the potential for expansion on our SQP-based model. Interactions between cyclists can be taken into account by varying the drag parameter. Along selected course profiles, climbers output lower power relative to their critical power roughly synchronously with time trial specialists. Environmental perturbations to the optimal solution had a greater effect on course elements with simplified downhill grades and humps.

Applying Optimal Control With SQP to Cycling Performance Represented by Constituent Course Elements

Contents

1 Introduction

In recent decades, the increasingly competitive landscape of cycling and advancements in bioenergetic models has led to a shift in focus towards developing power profiles optimized towards racers' strengths and physiological limits. Modern power monitoring systems which can be mounted on a bike allow riders to track their power output during the race and make informed adjustments that can improve their times beyond pacing alone. In the subsection of whole-body bioenergetic models which focus on the concept of critical power, there are a few key agreed-upon assumptions that the energy supply for human exercise is split into two components: capacity limited anaerobic energy, and rate-limited aerobic energy. There are 3 standard models typically referenced. The critical power model, first described in [1] involves a hyperbolic relationship between level of power output and the amount of time in which that power is able to be sustained. This relationship is often shown by plotting the level of power output against the time in which that power is sustainable (on a logarithmic scale). The levels of power output exhibits asymptotic behavior as the amount of time increases, suggesting that a certain power level would be sustainable for an infinite amount of time, termed the critical power (henceforth referred to as the CP).

For analysis within the scope of cycling, the critical power can be considered for the whole body rather than looking at fatigue from local muscular work. Given that CP is aerobic in nature, it is intimately related with a rider's lactate threshold and maximum oxygen uptake ($V_{02_{max}}$) [6]. The latter will be discussed later on.

The total energy spent above the CP level is limited by the anaerobic work capacity, henceforth referred to as W'. Research by Ferguson et. al [18] suggests that exhaustion of this capacity is reflected by human physiology through accumulation of key fatigue-inducing metabolites like inorganic phosphate and extracellular K^+ concentration which are present in chemical exchanges inherent to short-term high intensity muscle activity. With this, the power outputted by a person over the course of their exercise can be summarized by

$$P = \frac{W'}{t} + \text{CP} \tag{1}$$

given in [14]. The shortcomings and modifications of this model are discussed also in [14], as well as the 2 other largely accepted models for full-body bioenergetics: the 3-tanks model, first formulated in [2] and the Skiba model formulated in [21]. Both these models are modifications on the critical power model, accounting for different types of energy production in the body. The 3-tanks model describes recovery as a linear process, where $W'_{current} = W' - (P - CP)t$, however W' recovery kinetics have been demonstrated to be non-linear in nature and their aforementioned reflection in the body suggests that it cannot be represented as regaining of a simple source of stored energy. [18]. To avoid this simplification, the Skiba model introduces a recovery of W' over time, when performing under CP. After performing above CP for a given amount of work, W_{exp} this recovery can be modeled via the relationship

$$W'_{current} = W' - \int_0^t W_{exp} e^{-\frac{t}{\tau_W}} dt \tag{2}$$

Where t is the time spent since the power level has fallen below CP. It can be seen that as t increases, the exponential in the integrand will decrease, so the amount of energy available will increase.

In contrast, the expenditure of W' by the body can be effectively modeled as the product of power and time [1]

$$\Delta W' = \{P(t) - \text{CP}\}t \tag{3}$$

To characterize a specific power level, $\beta(t)$ is defined as a percentage of CP:

$$\beta(t) = \frac{P(t)}{\text{CP}} \tag{4}$$

Such that $\beta < 1$ represents the rider recovering, and $\beta > 1$ represents heavy-exertion and depletion of W'. We adjust our representation of expenditure to fit our model and include this factor:

$$W_{exp} = \int_0^t (\beta(t) - 1)\text{CP}(1 - \delta(t))dt \tag{5}$$

Here δt accounts for the difference between recovering W' and expending W' and is given by

$$\delta(t) = \begin{cases} 1 & \text{if } P \geq \text{CP} \\ 0 & \text{if } P < \text{CP} \end{cases} \tag{6}$$

The upper-end of a rider's power level is limited by their maximum power output which reduces over time while a rider stays above their CP. A rider operating at this power output is losing their W'

at the fastest rate and can only sustain for a short period of time before they exhaust this capacity. The transient maximum power can be modeled as proportional to the amount of W' at that instant

$$P_m(t) = CP + (P_{max} - CP)W' \qquad (7)$$

Where $P_m(t)$ represents the maximum power that the rider can output at any given time t during a race, while P_{max} represents the rider's true maximum power following a period of long rest which is inherent to the characteristics of the rider. The maximum power cannot be exceeded, therefore $P(t) \leq P_m(t)$ for all times t.

1.1 $V_{02_{max}}$ Relationship

In reviewing the literature, the importance of $V_{02_{max}}$is primarily seen as a representative indicator of an athlete's fitness. While it is inseparably related to CP, it is generally not an instrumental parameter in modeling a rider's power output for cycling. CP is generally agreed to represent not just the threshold above which anaerobic energy expenditure begins, but the highest sustainable work rate for which a steady state of V_{O2} uptake and elevated blood lactate and proton concentrations can be achieved [4, 17, 18]. This is consistent with Housh et. al. which demonstrated that there was little, if any, difference between the velocity at $V_{02_{max}}$and critical velocity (akin to CP)[5]. Other research analyzed by Billat demonstrated that the threshold for stable blood lactate levels exists at around 85% $V_{02_{max}}$, an intensity that athletes are consistently able to sustain for an hour. Above this, an athlete operating at their CP reaches and stabilitizes at 95% $V_{02_{max}}$[11]. A time limit of 30 minutes or less at this sustained level of exertion is imposed by rapid glycogen depletion. Reported data from 32 individuals in a study by deVries et. al. concluded that the mean CP (230W) was significantly higher (28%) than the mean power output associated with the blood lactate threshold, strengthening the case for existence of this limit [3]. While highly relevant to longer-format cycling competition, we will assume that this limit cannot be reached and that CP can be sustained indefinitely, as will be discussed later in the assumptions.

By the time a rider exceeds their $V_{02_{max}}$, they are also exceeding their CP and depleting W'. For short bursts of high intensity exercise, recovery rates for $V_{02_{max}}$have been shown to exceed that of W' and therefore do not serve as a limit to throttle the rider's power level [18]. Edge cases where a rider enters a long and extremely steep incline following a downhill during which W' has been almost fully recovered may result in the rider ultimately being forced to throttle their power from exceeding their $V_{02_{max}}$. For these edge cases, our model which does not include transient V_{O2} falls short of predicting the optimal strategy.

2 Cyclist Profiles

We consider elite cyclists registered as competitors sanctioned by the Union Cycliste Internationale (UCI). The cyclists considered identify either as time trial specialists or climbers and as either female or male.

2.1 Time Trialist

A time trial specialist is someone who excels at medium to long distances with little to no grade. They are typically heavier in weight and able to maintain a consistent strong pace over long relatively flat courses. An experienced time trialist trains to increase CP and output power just below their CP for the majority of the race to maintain pace [20, 30, 33]. Because they spend less time above CP, it would be expected that anaerobic reconstitution would take place slower, giving rise to a larger τ_w.

2.2 Climber

The climber excels with long and high grade slopes, exhibiting repeated bursts of acceleration uphill. The environment lends itself toward individuals having a lighter weight to reduce the force they are fighting up inclines [9, 12, 16]. It would then be expected that a climber would comparatively spend more time above CP during climbs and recovering during downhills from exerting anaerobic work. Furthermore, expectations would point towards faster recovery times for rapid hills, and thus a smaller τ_w. Because ideal pacing for a climber is more variable throughout the course, having a higher CP as well as P_m is less important compared to being able go above CP more frequently.

3 Model Parameters

Based on the formulation given in [28], we consider the forces that the rider must generate in order to continue riding. This includes opposing air drag, $F_d = C_d(v + v_w)^2$ where v is the rider's velocity and v_w is the headwind velocity. The resistance due to the slope of the track at that point is given by the sum of the gravitational force parallel to the incline as well as the rolling resistance from the wheels, namely $F_r = mg(\sin\phi + C_r)$ where ϕ is the slope of the track at that point and C_r is the resistance coefficient for the cycle. The time and environmental dependence of the resistance is not considered. Together this is

$$F = C_d(v + v_w)^2 + mg(\sin\phi + C_r) + m_e\frac{dv}{dt} \quad (8)$$

where m_e is the effective mass of the rider, accounting for the kinetic energy of the rotating wheels. For initial results, the configuration of the track is solely taken into account via ϕ. Considerations due to turns in the track are discussed later in section 4.3.2. A more detailed model of rider completion times taking into account turns and drive train efficiencies is given by [24].

The following physiological and physical characteristics will be used to define and distinguish the two types of cyclists:

- Critical Power CP[W]
- Anaerobic Work Capacity W' [kJ]
- Maximum Power P_{max} [W]
- Rate of recovery τ_w [s]
- Drag Area C_dA [m^2]
- Body weight [kg]

Based on the descriptions of each type of cyclist discussed in section 2, the model parameters were either taken from literature (when available) or determined via tuning our model to achieve the desired behavior (i.e. the time trial specialist will always beat the climber in a long, flat course, etc.). Data found in the literature was taken from [16] and [9]. The values for these parameters used are shown in table 1.

Type of Cyclist	CP [W]	P_m [W]	m [kg]	W_{cap} [kJ]	τ_w [s]	C_dA [m^2]
Male TT specialist	357 ± 18	450 ± 30	71 ± 4	22 ± 1	2000 ± 1500	0.35 ± 0.02
Male climber	320 ± 10	398 ± 20	62 ± 5	45 ± 2	10 ± 50	0.33 ± 0.01
Female TT specialist	282 ± 19	363 ± 30	61.6 ± 3	17.5 ± 2	2000 ± 1500	0.318 ± 0.02
Female climber	250 ± 20	310 ± 18	54 ± 2	31 ± 2.5	10 ± 50	0.30 ± 0.01

Table 1: Rider Profile Parameters. Range of parameter specified is the range in which the model still exhibits expected behavior for that cyclist type.

A detailed study of the models sensitivity to these parameters in terms of the qualitative behavior of optimal solutions is given in section 6.

4 Model Formulation

4.1 Goals

A model seeking to optimize a rider's power output during a course will be bounded by their

CP, W', u_{max}, and τ_w their time taken to recover (referred to as the 'time constant of reconstitution in [29]). A rider should increase their power output for climbing steep inclines and passing opponents and recover anaerobic capacity on downhills and straightaways. The optimization model should seek to determine the ideal power output that will maintain a stable amount of W', i.e. leaving enough energy 'in the tank' to avoid having to limit output at or below the CP during strategic sections of the course. Current literature highlights the importance of the 'kick' at the end of a race for a rider to use all their remaining anaerobic energy to speed towards the finish line. Although additional considerations can be made into applying greater weighting to this end portion of the race, these considerations are beyond the scope of this model, and the fundamental goal of ending the race with zero W' remaining as implemented is crucial for any model generating a rider's power profile regardless of the race category.

4.2 Optimal Power Output

The problem of finding the most optimal power output over the course of a race can be framed as an optimal control problem, as is done in [28] and [25]. Both papers use the relationship between force, power and velocity given by $P(t) = F(t)v(t)$ to recast the problem of finding an optimal power curve to finding an optimal velocity curve. This is useful because it formulates the problem as finding a function $v(t)$ that minimizes the functional given by

$$\int_0^L \frac{1}{v(t)} dx = T_f \tag{9}$$

Once this optimal $v(t)$ is found, we can use equation 8 to find $P(t)$. This problem will be subject to the constraints that $P(t) \leq P_m(t)$ where P_m is given by equation 7 and that

$$W'_{capacity} - \int_0^{T_f} W_{exp} e^{-\delta(t)\frac{t-u}{\tau_w}} dt = 0 \tag{10}$$

Where $t - u$ is the time since going below CP.

The second constraint comes from equation 2 and the assumption that W' is completely depleted at the end of the race such that anaerobic energy has been fully utilized by the rider. W_{exp} is similarly given by equation 5. These constraints differ from [28] and [25] in that they account for recovery of W'.

The addition of this nonlinear and discontinuous recovery term (discontinuous due to $\delta(t)$) makes the optimal control problem significantly more difficult to solve in the way shown in [28] and [25]. However, optimal control problems such as this can be solved via sequential quadratic programming (SQP) methods by discretizing the problem [7, 10, 22]. This approach is taken to circumvent these problems.

4.3 Application to Specific Time Trials

The model was applied to 3 different time trial courses: the 2021 Tokyo Olympic Time Trial (22.0km), the UCI World Championships in Belgium (48.7km), and a constructed square course consisting of four rises and falls with a mathematically imposed radius of curvature of 10 meters around each bend. The men's Tokyo Olympic Time Trial course consists of two laps on the same track compared to one lap for women. To minimize the time taken to compute the model, the women's course is utilized with the expectation that results will be comparable to the men's course.

In the absence of environmental perturbations, the optimal path over the entirety of the 2021 Tokyo Olympic Time Trial and the UCI World Championships in Belgium were found from this base model. Parameter values were selected as typical values within the range expected. Section 6 describes the sensitivity of the model to these parameters. The results of these simulations are shown in figures 1 through 6.

4.4 Environmental Perturbations

There are three environmental perturbations incorporated into the model:

1. Changes in the drag force experienced due to wind

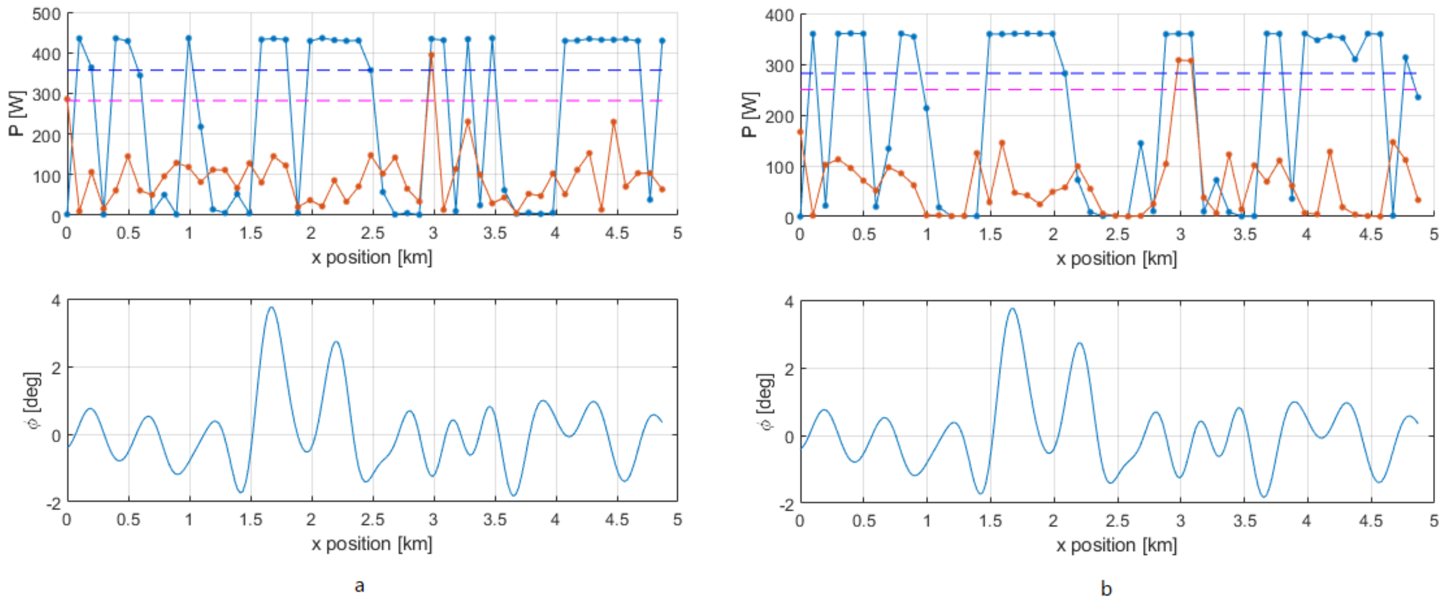

Figure 1: Optimal power output (upper subplot) for the associated ϕ (lower subplot). Data reflects parameters for the time trial specialist (blue) and climber (red). CP value for time trial specialist shown as dark blue dotted line, and CP value for climber shown in magenta dotted line. The values of ϕ went through a low pass filter to smooth out jaggedness from the initial calculation of the grade. ϕ values calculated from the 2021 UCI World Championship course. Plot (a) is data taken for male cyclist, plot b is data taken for female cyclist.

2. Changes in the resistive forces from the track due to turning

3. Changes in the force of gravity on the rider due to the grading

Perturbations 1 and 3 are already incorporated into equation 8.

4.4.1 Wind Perturbations

The original formulation of equation 8 from [28] contained a term for variations in the drag force due to wind, but it was neglected and set to 0 to simplify the model for analysis. Because of our alternative technique for solving the optimal control problem, we can include this term.
To account for the direction of the wind on the track, v_w (from equation 8) was calculated via

$$v_w = v_{mag} \cos\beta \tag{11}$$

where v_{mag} is the magnitude of the wind's velocity and β is the angle between the rider's heading and the wind direction. A similar implementation of the wind's affect on cycling output was implemented in [15]. The angle β can be calculated from the map of a track, assuming that the rider will always have their heading tangent to the track at that point. This was done for each of the tracks studied; an example of which is shown in figure 8. It is worth noting that β is calculated for an arbitrary constant direction throughout the length of the track, so it is assumed that the wind points in a constant direction throughout the ride.

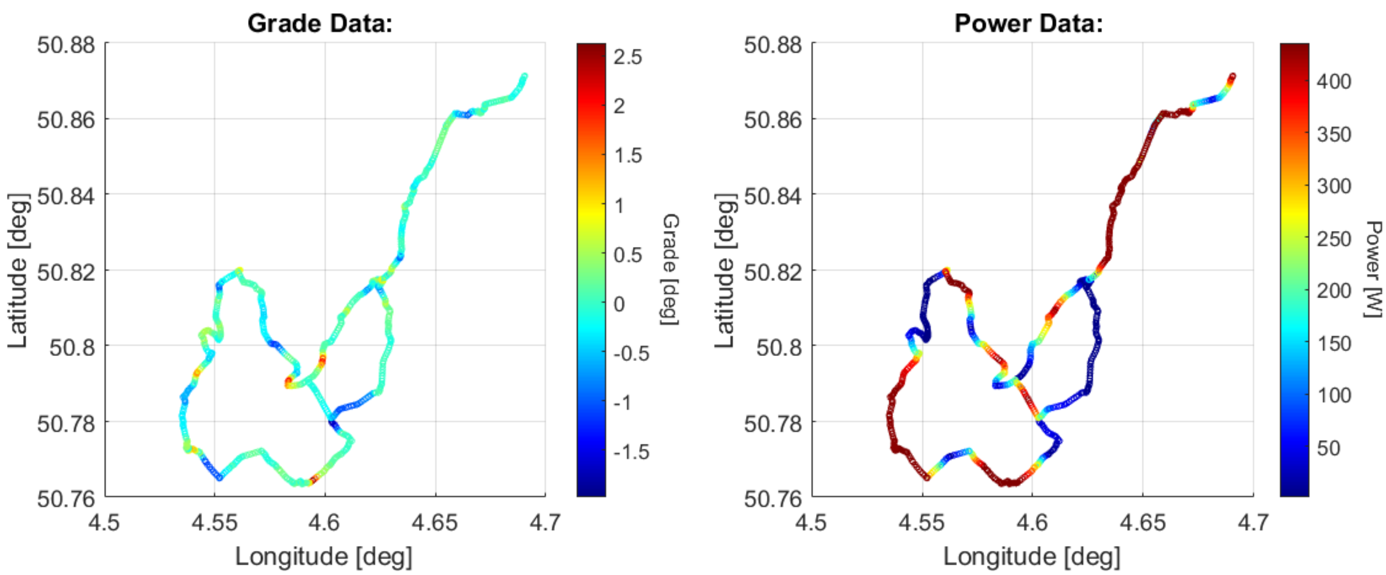

Figure 2: Optimal power output for the 2021 UCI World Championship course for a male time trial specialist. Power data is that of Figure 1.

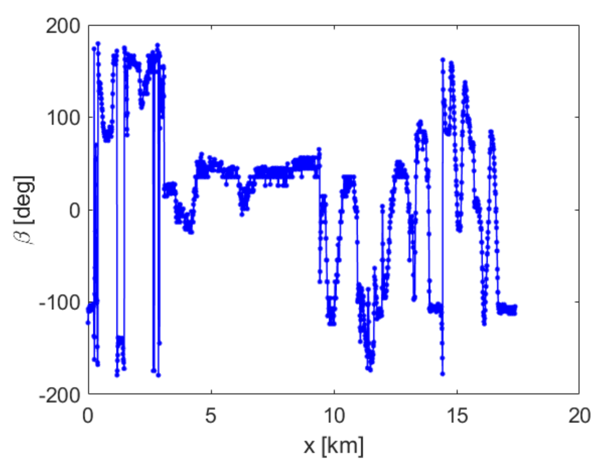

Figure 8: β was calculated based on track lat/lon for the Tokyo 2021 Olympic Time Trial Course.

4.4.2 Curvature of the track

It is assumed that all turns are banked turns, meaning that the seen effect on the biker is that the normal force from the ground on their wheels is increased by an amount proportional to $\cos\alpha$ where α is the angle between the vertical gravitational force (mg) and the horizontal centripetal force ($\frac{mv^2}{r_c}$). A similar technique for account for curvature of the track was implemented in [24]. Thus we accounted for this curvature by adjusting our coefficient of wheel resistance (as the frictional force would be proportional to the normal force).

4.4.3 Grade of Accent/Decent

The grade of the track is given at every point by ϕ, and affects the forces by equation 8. For both the Tokyo 2021 Olympic time trial and 2021 UCI World Championship course, ϕ was calculated at every point by the change in elevation. Due to discretization of the elevation data, the data was very jagged with many sharp, quick changes. The lack of smoothness in these values adversely affected the stability of numerical solutions, so the values were fed through a low pass filter. The cutoff frequency of this filter was empirically found.

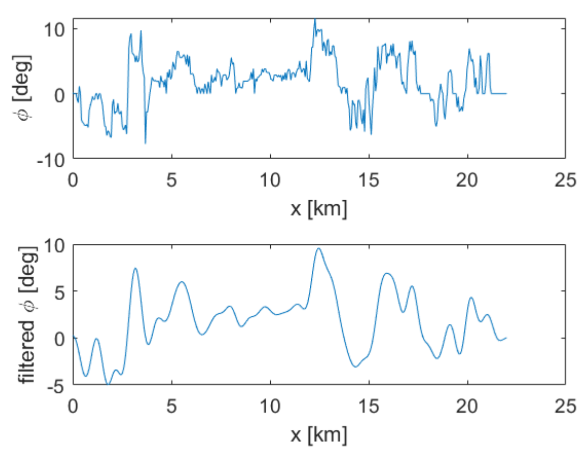

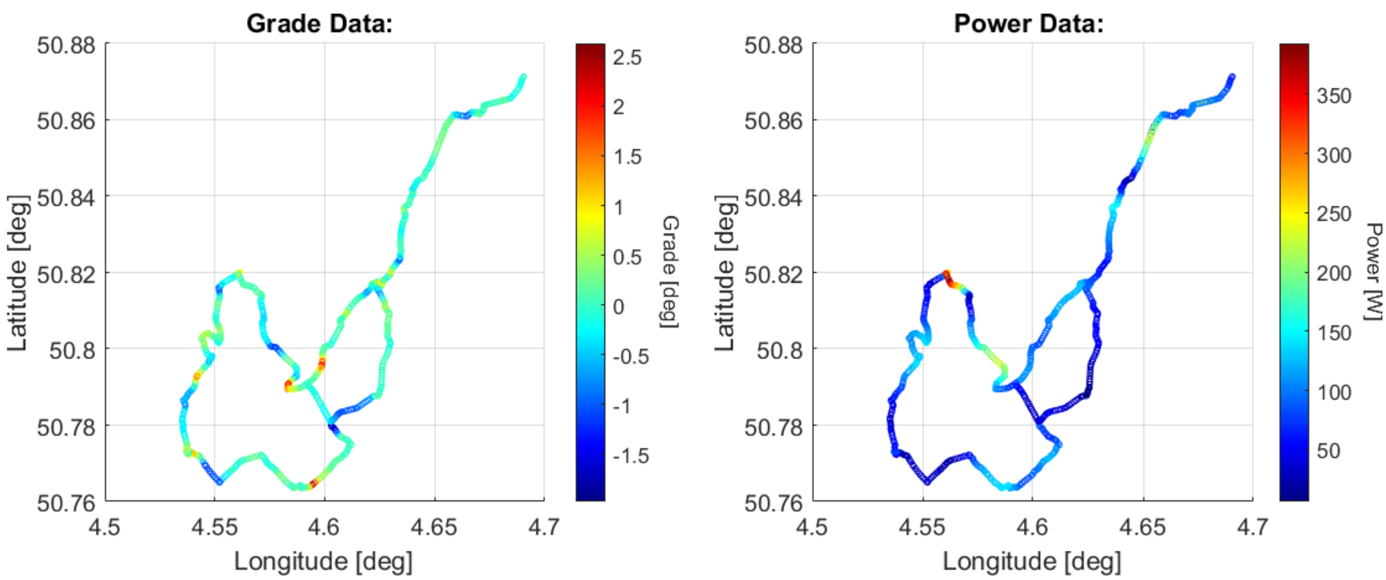

Figure 3: Optimal power output for the 2021 UCI World Championship course for a male climber. Power data is that of Figure 1.

Figure 9: ϕ calculated from the Tokyo Olympic course in upper plot and the same data after going through a lowpass filter.

4.5 Assumptions and Limitations

Most fundamental to our formulation of the problem is our assumptions of the model's perfect knowledge of both the velocity and power between different spots along the track. This allows us to optimize the velocity and power over the whole course of the race at once, rather than determining the optimal path as that path is executed. The model is thus more useful as a means of planning a race beforehand, in situations where there is little uncertainty with the specifications of the track. The alternative is a model that could adaptive determine the optimal "next move" based on the current state. A similar idea is discussed in section 7 on the method of course elements.

The inefficiencies in the drive train of the cyclists crank and wheel barrings are ignored. Other models focused more on the interactions of the cycle itself, such as [24] take this into account as a scaling factor in their applied power from the cyclist. For the purposes of this paper, it is assumed that the drive chain is efficient enough for its effects to be negligible.

In [29], the accuracy of the τ_w model for exponential recovery of W' is discussed and it is found that it can misinform the recovery of W' for non-elite athletes. Thus, our model is only applicable for elite cyclists who are high performing. This is not restrictive because we are only considering cyclists that have been competitors sanctioned by the UCI.

Before using the values of ϕ calculated from the course data, a low pass filter was applied to smooth out the jaggedness. The reasons for this are discussed in section 4.3.3. Due to the nature of low pass filters, short term variations in the grade was ignored after the low pass filter was applied. Thus, in courses where a high degree of variance in the grade over small length scales is significant, our model would not accurately represent the course. Our model is more suited for handling situations where short-term oscillations are not significant and only slower more gradual changes in the grade are significant.

Although social and socio-economic backgrounds of the cyclists is significant in decision making and thus influential to performance, interpersonal interactions investigated in this model will not be correspond to the backgrounds of individual cy-

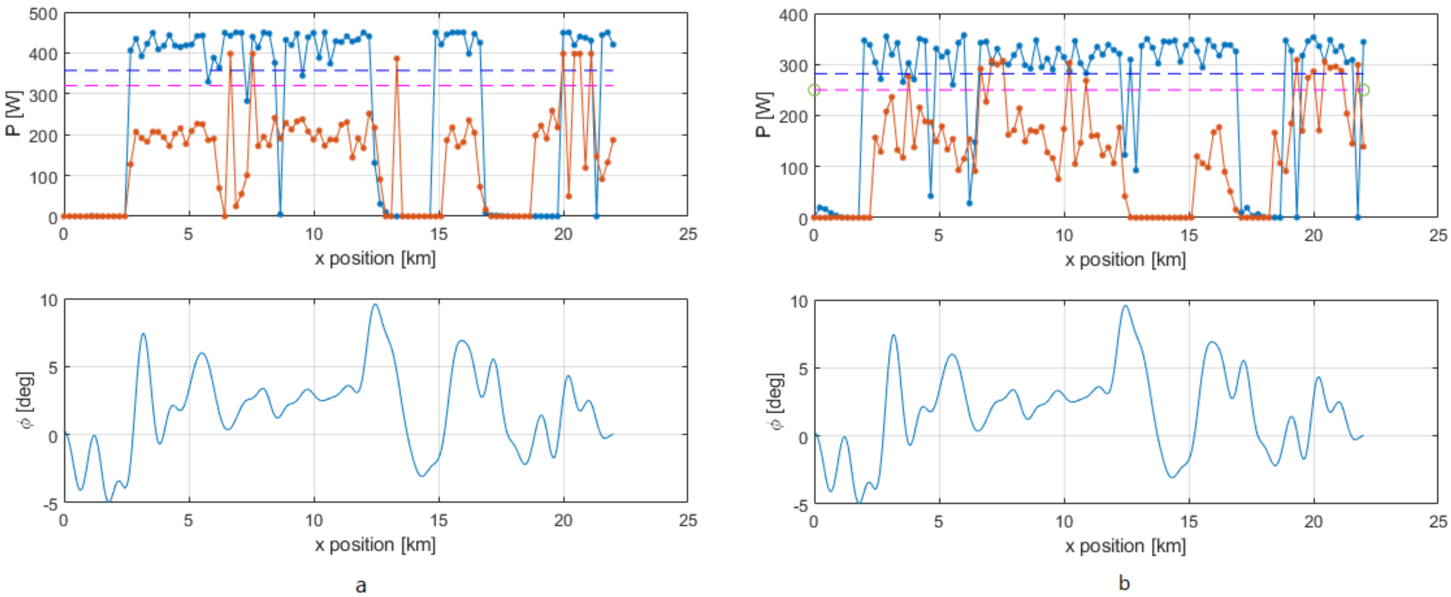

Figure 4: Optimal power output (upper subplot) for the ϕ shown in lower subplot. Data reflects parameters for the time trial specialist (blue) and climber (red). CP value for time trial specialist shown as dark blue dotted line, and CP value for climber shown in magenta dotted line. The values of ϕ went through a low pass filter to smooth out jaggedness from the initial calculation of the grade. ϕ values calculated from the 2021 Tokyo Olympic Time Trial course. Plot (a) is data taken for male cyclist, plot b is data taken for female cyclist.

clists [32].

4.5.1 Environmental Simplifications

In considering perturbations caused by the conditions of the track, weather, and environment, simplifications were made. Temperature influences the aerobic efficiency of athletes resulting in longer finishing times on hotter days when athletes must spend more energy to cool their bodies. For venues which are located above sea level, altitude plays an increasingly important role in decreasing an athlete's $V_{02_{max}}$ due to the lack of available oxygen in the atmosphere. At a certain point well above sea level, $V_{02_{max}}$ will function as an upper limit on pacing instead of CP. As discussed in [27], rain and snow conditions can cause slick or muddy conditions which have a significant affect on track times as riders must reduce their speed to avoid losing traction. Additionally, long races will have some of these condition change over the course of the race due to changing weather, large altitude gains, and even changes altering the mechanical efficiency of the cycle. These perturbations all represent conditions which are difficult to predict prior to a race and/or negligible in effect compared to perturbations discussed later in 6.1. It is therefore reasonable to neglect these perturbations in pursuit of a model which can be executed within reasonable time and focuses on a more general optimal solution rather than live-updated guide. Wind blowing normal to the path of the biker is assumed not to impact biking performance.

4.5.2 Course Topography

Power profile is closely related to topography and size of the course. Longer and more steep courses would require different strategies than that of a of short flat course (such as a time trial). This was taken into account both in the grade of ascent the rider is subjected to (ϕ) and the radius

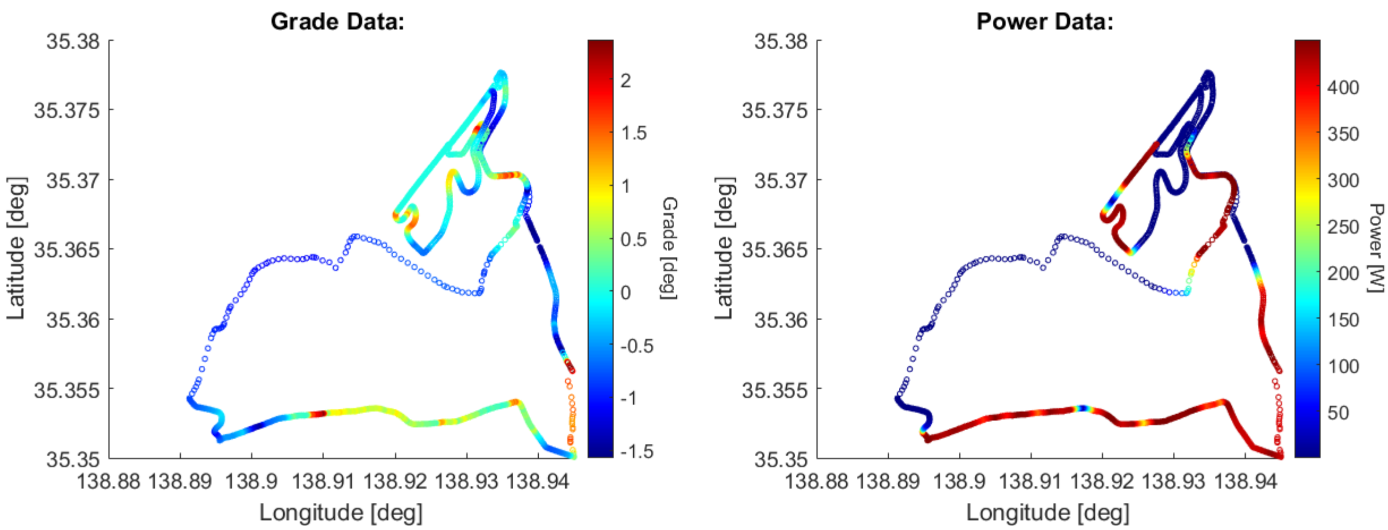

Figure 5: Optimal power output for the 2021 Tokyo Olympic Time Trial course for the time trial specialist with power data in figure 4.

of curvature of the track (r_c), both varying with the riders position along the track.

4.5.3 Rider to Rider Interactions

Although some disciplines of professional cycling feature isolated individuals during a race, may feature cases were teams or multiple competing individuals are present on a track at the same time. In these cases, interactions between riders can have significant impacts on the achieved final time. Our model model neglects these interactions and only considers a single rider, on the track alone.

One primary component of these interaction is known as drafting, where rider trail in the aerodynamics wake of other rider to reduce drag and thus conserve energy. The implications of extending our model to include drafting are discussed in section 9.

5 Model Validation

5.1 Power Output Grade

Results from our model indicate that the power level at any point in the race for both types of riders is closely tied to the grade of the track at that point. As the grade increases, the model increases the power output. This is especially visible in figure 4 given that the Tokyo track has a long climbing section. For the time trialist, the power output is shown to increase above their CP during steep grades, often to the maximum power, and drop to zero during downhills, indicating that W' is being recovered during the downhill sections. Climbers also demonstrate a trend of increasing in power during steep grades but with less consistency, rarely going above their CP. Possible explanations for this behavior will be discussed later on.

These results show a clear preference towards a variable power output towards minimizing times and that it is advantageous to respond to the environment, particularly for the climbers. This closely aligns with findings from Cangley et. al [19] that a variable power output can result in 2.9% time savings over a 4km course. Furthermore, Gordon [13] and Skiba et. al. [21] assert that putting the most effort into climbing sections will optimally decreases track times, as is demonstrated by our model. During flatter parts of the course with less variation in grade, the power output tends towards stability rather than fluctuation as this is the ideal strategy for a flat course. [31]

One might question whether the strategy for

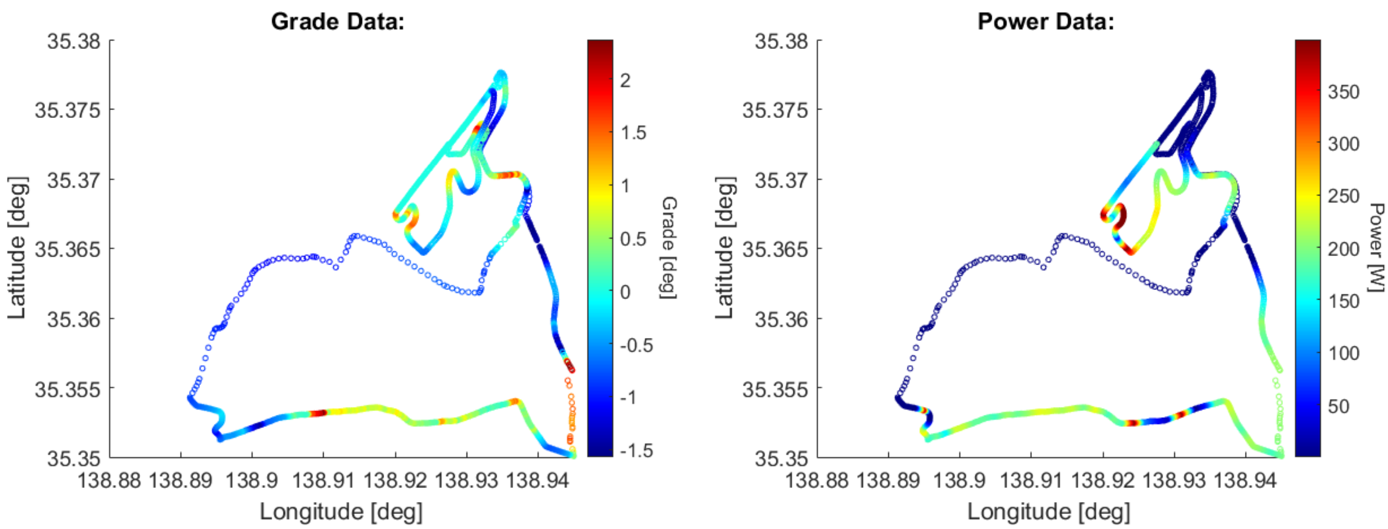

Figure 6: Optimal power output for the 2021 Tokyo Olympic Time Trial course for the climber with power data in figure 4.

time trialists found by the model lacks moderation by consistently being nearly full power or zero power. Sundström et. al. evaluate optimization strategies from two models, CPIE and M-M; the response from CPIE is very similar to our model output, significantly exceeding CP and dipping below during hills, whereas M-M suggests a more moderate approach, starting off well above CP and decreasing throughout the course (similar to the ubiquitous 'all-out' pacing strategy) [23]. The CPIE model resulted in a strategy that was 0.68% faster than M-M, indicating that our model tends towards a highly optimized yet sensitive strategy which may be less feasible to execute for a rider.

5.2 Time Trialist vs Climber Performance

Time Trialists demonstrate a clear advantage over climbers in performance for both the Tokyo course and Flanders course with faster finishing times for both males and females. The best performance displayed is on the Tokyo track during a long uphill section in the course. In this particular section of the course, a climber's specialized physiological make-up is better equipped to perform well than the majority of the course in Flanders. The solution for climbers suffers from noise more than time trialists. Some of these characteristics are likely a result of numerical instability and shortcomings of the model, evident by the increased noise in the power output for climbers compared to time trialists. Climbers stay below their CP for nearly the entire portion of the course, demonstrating an under utilization of energy. One possible explanation for this may lie within the choice of parameters, specifically that setting τ_w to 10±50 seconds may be too low. As discussed by Bartram et al., as the limit of τ_w approaches zero, D_{CP} approaches infinity, where D_{CP} represents the mean difference between CP and the work rate during a portion of recovery [29]. In other words, for very high values of D_{CP}, the model significantly dips below CP to recover W' beyond a point that would be considered optimal. This effect is sustained because neither the Tokyo nor Flanders track contains grades significant enough for the model to warrant going above CP.

Increasing τ_w to resolve this problem proves to be challenging as the model output is not qualitatively changed from the time trialist with values of τ_w above 200s. This limit is discussed more in the Model Sensitivities section, and proves to be a shortcoming of our model. Increases in power output for the climbers also appears to be out of

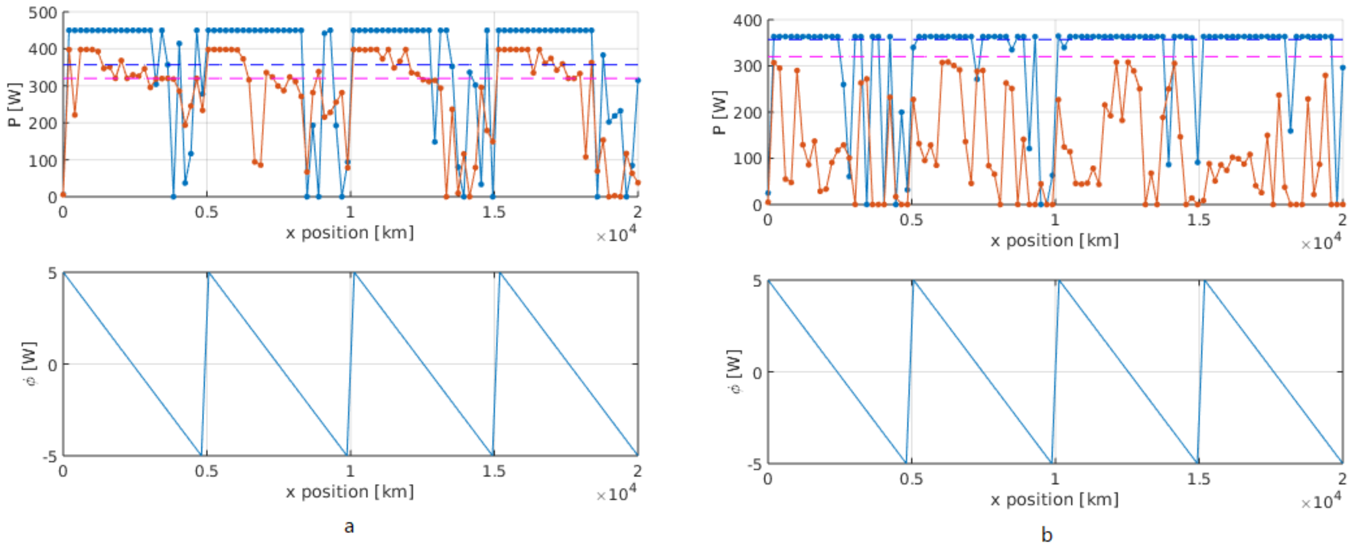

Figure 7: Optimal power output (upper subplot) for the ϕ shown in lower subplot. Data reflects parameters for the time trial specialist (blue) and climber (red). CP value for time trial specialist shown as dark blue dotted line, and CP value for climber shown in magenta dotted line. The values of ϕ went through a low pass filter to smooth out jaggedness from the initial calculation of the grade. ϕ values calculated from a course of our own design. Plot (a) is data taken for male cyclist, plot b is data taken for female cyclist.

phase at times with uphill sections of the course. This can be detrimental to maximizing the utilization of a riders energy as varying power at a frequency less than or greater than the features of the course is shown to produce slower track times [26]. Regardless, the more general conclusion that climbers are less competitive than time trialists on tracks without significant grades is in agreement with our expectations and literature. A climber's power curve is less optimized for these two courses than that of a time trialist.

Several studies found use alternative methods for arriving at an optimized power distribution curve in simplified track conditions[8, 13, 24, 25, 28]. We compared out model to each of these finding some similar trends.
The solution found analytically in [25] and [28] matches our numerical solution closely in shape for the case of a perfectly flat course.

6 Model Sensitivity

Convergence of an optimal solution to the control problem was studied initially for a simplified situation of a nearly 0-grade single rider situation. Different rider and course parameters were studied individually to inform the level of fidelity needed in those parameters as well as our partitioning of the space of rider parameters. The parameters studied and their sensitivity are given in table 2. An important note is that while some of the parameters (such as the rider mass) did not drastically affect the model output within it's range, it did affect convergence time. The critical power, CP was found to have little affect on the qualitative model behavior below a certain value. So above 180W, the model is very sensitive to CP but below 180W, the effect of changing CP is a shift in the power level over the entire course of the race. This effect is visualized in figure 10. This is expected to be due to the interaction between the W' expended and the maximum velocity. When the rider can work at higher power values while staying below W', they are more limited by their maximum possible velocity (and their maximum power output, as we would predict) and air drag. This makes the optimal control problem more difficult which can lead to more complex behavior and possible instabilities in the solution.

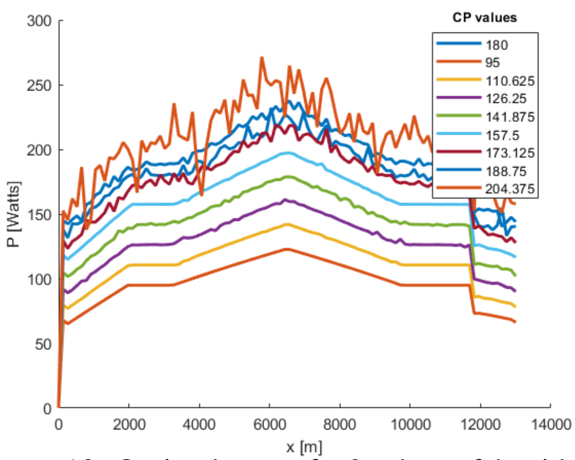

Figure 10: Optimal power for 9 values of the rider's CP.

Varying $W'_{capacity}$ was found to have little affect on the optimal strategy found. This would mean that, although the times taken to complete the course would be different, the optimal strategy would be the same regardless of one's $W'_{capacity}$. This may not be the case for a more complex course profile (namely, one where the grade would be subject to more change).

Similar to CP, the maximum power of the rider was seen to have little effect on the optimal strategy beyond a certain value. This is expected because in most optimal power curves the power was always well below the maximum. So in most case (those in which there is a big separation between CP and P_m is large) this is not a limiting factor of the ride.

The model's qualitative dependence on τ_w was found to be that only below a certain threshold (200s) did it's value change the shape of the optimal solution. We hypothesize from this that reconstitution of W' related to τ_w does not become a significant factor when slow enough in the case of a straight track.

6.1 Sensitivity to Environmental Perturbations

6.1.1 Effects of wind

Variation in the magnitude of the headwind was tested on the Tokyo Olympic course was found to slightly vary the power between the maximum and minimum value in a given section, but not to change the value of those maximums and minimums. There was still a trend between the distribution of power and the grade of the course, but significant variation in the way in which the rider responded to grade variations was introduced. We hypothesize that the seemingly random nature of these variations comes from the complex motion of β throughout the course, shown in figure 8.

The results on average power delivered by the rider and time taken to complete the course can be seen in figure 11, following no discernable trend. Additionally, wind patterns are often unpredictable in practice and both the magnitude and direction of the wind will like change in unpredictable ways throughout a race. Thus, the most effective way to assess the effect of wind on the the optimal solution is to examine it statistically. This is done in section 7.6.1 on the course elements.

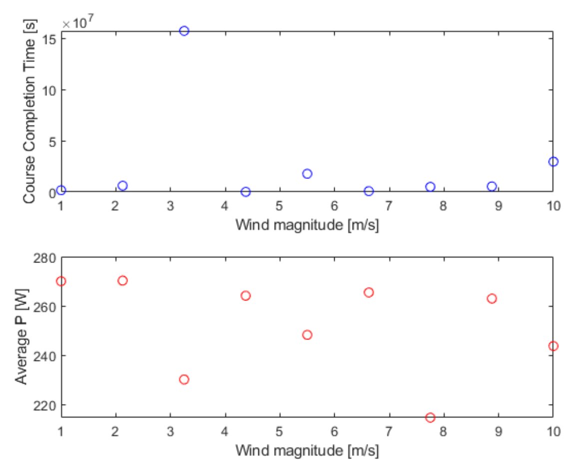

Figure 11: Completion time and average power output for 9 different headwind magnitudes. Course data was from the Tokyo 2021 Olympic time trial course and the male time trial specialist profile was used.

6.1.2 Effect of track curvature

Similar to wind, the effect of track curvature in the data from figures 1 to 6 was seen to be analogous to adding noise due to its continuous variations on small scales. Unlike wind where uncertainty in the perturbations is likely, the rider will likely have precise knowledge of the track curvature before the race. Thus, we studied the effect of specific track curvatures in certain conditions, such that we can generalize to arbitrary tracks. This is discussed in section 7 and 7.6.2.

6.2 Effect of Rider Deviations

A realistic rider will not be able to follow such a sharp and discontinuous power distribution plan as we have outlined. In actuality, a riders power distribution will have smooth trends with smaller, high frequency noise, such as the data used in [24]. Ignoring these higher frequency variations in the power distribution, we can approximate a more realistic with some smoothing of the data via a lowpass filter. To first order, the smoothing of P will be equivalent to a proportional smoothing in v. The effect of this smoothing in v on the completion time for the Tokyo course is shown in figure 12. The drastic effect at cutoff frequencies near the sample frequency is likely to due sample errors. Sampling below $0.2 f_{sample}$ caused convergence of the completion time to near it's original value. This trend was seen in other sample solutions taken as well. A more extensive study of this effect could involve propagating v via a differential equation in terms of the applied power, as is done in [24].

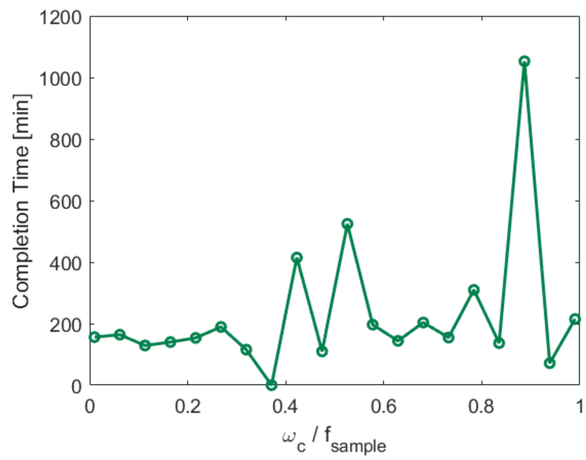

Figure 12: A sample optimal solution for the Tokyo Olympic course was smoothed via a lowpass filter with varying cutoff frequencies (ω_c) as ratios of the sample frequency $_{sample}$. The solution comes from biker parameters consistent with the male time trial specialist.

Parameter	Symbol	Typical Value	Units	Range
Rider mass	m	58	kg	± 13
Critical Power	CP	180	W	≤ 190
Anaerobic work capacity	$W'_{capacity}$	25000	J	± 20000
Maximum Power	P_m	350	W	$\geq$ CP + 40
Anaerobic recovery time constant	τ_w	500	s	± 300
Drag area coefficient	$C_d A$	0.35	m^2	± 0.4

Table 2: Initial Sensitivity to model parameters

7 Course Elements

To generalize the model's output to an arbitrary course structure, we can approximately break up a given course into "course elements", that are short basic building blocks which can be concatenated in order to make an arbitrary track. Our model can be studied on each of these basic course elements and optimal solutions to a concatenation of these course elements can be well approximated as a concatenation of optimal solutions to each of the elements. This is a similar method to that employed by [13], finding solutions to several simplified courses in order to extrapolate an optimal solution to a general course.

7.1 Element 1: Straightaway

The straight away element is a stretch of track with no incline. It's power curve is given below in figure 13. These results for a rider on a straight are qualitatively supported by those found in de Jong et al. 2016, where the power output for a racer was modeled analytically along a flat track of the same length shown in figure 13. Both display a sharp initial incline in applied power follow by a short dip and then relatively constant output for the remainder of the track [25].

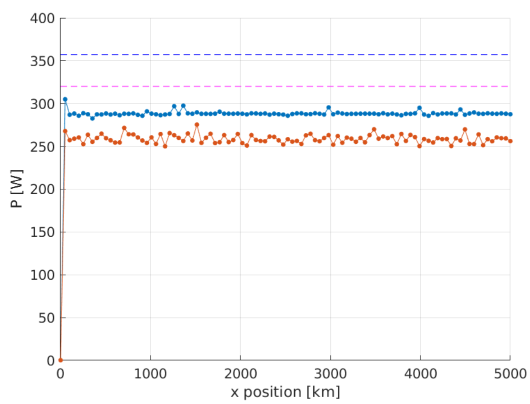

Figure 13: Model generated optimal power output along Element 1. The parameters used were those of the female time trial specialist (blue) and female climber (red). The value of CP for the time trial specialist is plotted in the dark blue dotted line. The value of CP for the climber is plotted in the magenta dotted line.

7.2 Element 2: Upward Grade

Element 2 consists of a upward grade simulated as a constant positive ϕ of 5 degrees. The optimal power output qualitatively closely matches the trends observed in that of element 1.

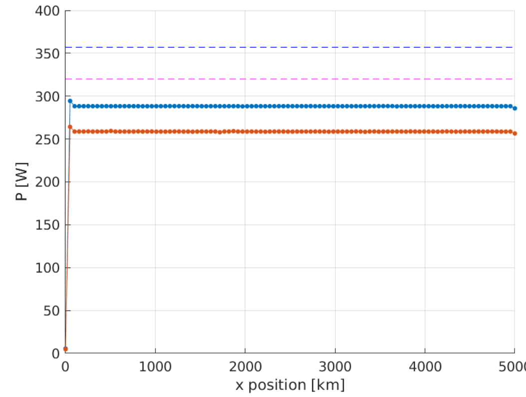

Figure 14: Model generated optimal power output along Element 2. The parameters used were those of the female time trial specialist (blue) and female climber (red). The value of CP for the time trial specialist is plotted in the dark blue dotted line. The value of CP for the climber is plotted in the magenta dotted line.

7.3 Element 3: Downward Grade

Element 3 is the downward grade compliment to element 1 with a slight modification. Instead of being simulated with a constant negative ϕ of -5 degrees, the model consist of 3 equally sized sections of $\phi = 0$ degree grade followed by a $\phi = -5$ degree grade and then another $\phi = 0$ degree grade. This modification is to allow for improved chance of convergence from random initial conditions.

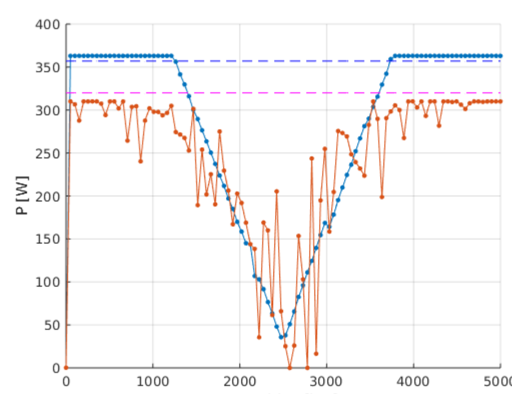

Figure 15: Model generated optimal power output along Element 3. The parameters used were those of the female time trial specialist (blue) and female climber (red). The value of CP for the time trial specialist is plotted in the dark blue dotted line. The value of CP for the climber is plotted in the magenta dotted line.

7.4 Element 4: Positive Hump

The positive hump was simulated as a linear decrease in ϕ from 0 to -5 degrees in the first half of the element followed by a linear increase in ϕ from -5 to 0 degrees in the second half of the element.

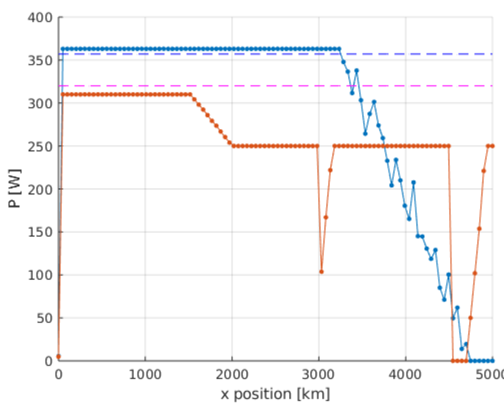

Figure 16: Model generated optimal power output along Element 4.The parameters used were those of the female time trial specialist (blue) and female climber (red). The value of CP for the time trial specialist is plotted in the dark blue dotted line. The value of CP for the climber is plotted in the magenta dotted line.

7.5 Element 5: Negative Hump

Like the positive hump, the negative hump was simulated as a linear increase in ϕ from 0 to 5 degrees in the first half of the element followed by a linear decrease in ϕ from 5 to 0 degrees.

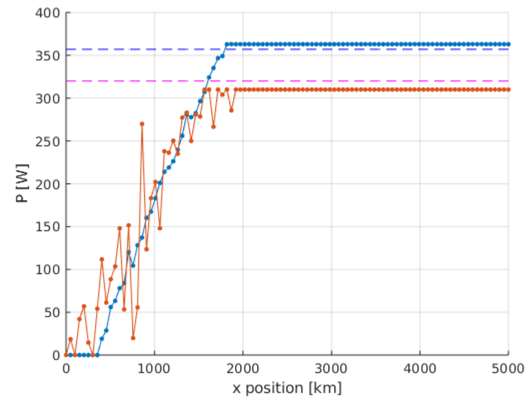

Figure 17: Model generated optimal power output along Element 5.The parameters used were those of the female time trial specialist (blue) and female climber (red). The value of CP for the time trial specialist is plotted in the dark blue dotted line. The value of CP for the climber is plotted in the magenta dotted line.

7.6 Environmental Perturbations on Course Elements

7.6.1 Effect of Stochastic Wind

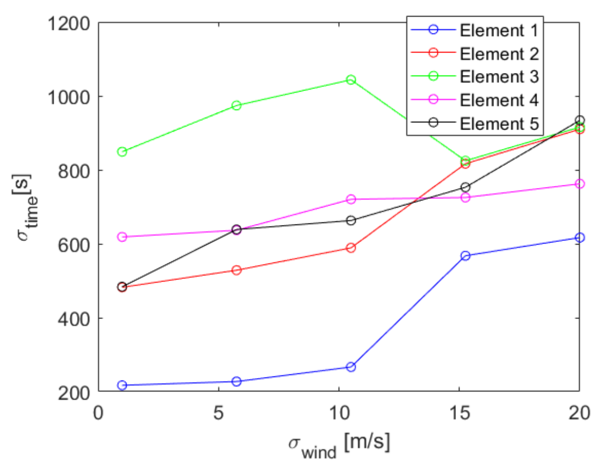

Figure 18: Effect of added stochastic wind at a given standard deviation. Standard deviation of time (y axis) is found by running the model 5 times with randomly generated wind headwinds with standard deviation σ_{wind}.

Shown in figure 18, the relationship between the standard deviation of headwind and the standard deviation of the completion times is close to linear for each element, up to between 10m/s and 15m/s.

At this point, each of the element's relationship changes. The downward grade's optimal solution is affected less after this point. Both the upward grade and the straightaway are affect more after this point. The positive hump shows this qualitative change the least, and in general is affect least by increased headwind.

It is hypothesized that the point between 10m/s and 15m/s is a point in which the wind is able to overpower the biker's velocity contributing more to the drag terms. Thus, the point at which the wind's variability would be more significant likely dependent heavily on the parameters of the rider and their velocity throughout the race. For riders with parameters near that of the male time trial specialist studied, the speed at which wind variation becomes a more significant perturbation is approximately 12m/s.

7.6.2 Effect of Track Curvature

For sufficiently small track elements, the radius of curvature can be treated as constant. Thus, we can make generalizations about arbitrary track curvatures by studying the effect of various constant radii of curvature on the track elements. This was done for our 5 course elements, the results of which are shown in figure 19. As expected, for large enough radii of curvature, there is little effect on the completion time or the average power.

Like in the study of stochastic wind on the course elements, it is found that the straightaway and the upward grade exhibit similar responses to these environmental perturbations. We can also observe that these two course elements showed the least variation due to track curvature. We can then conclude that optimal solutions for courses with a higher concentration of the other 3 elements (the downward grade, the positive hump and the negative hump) will be affected more by high degrees of curvature compared with courses that have a higher concentration of elements 1 and 2.

The same study done instead for biker parameters consistent to the male climber similarly yielded the same trends between the straightaway and upward grade course element. There was significantly less deviation for all course elements in terms of completion time for the climber suggesting that the climber's optimal strategy is less affected by this environmental perturbation.

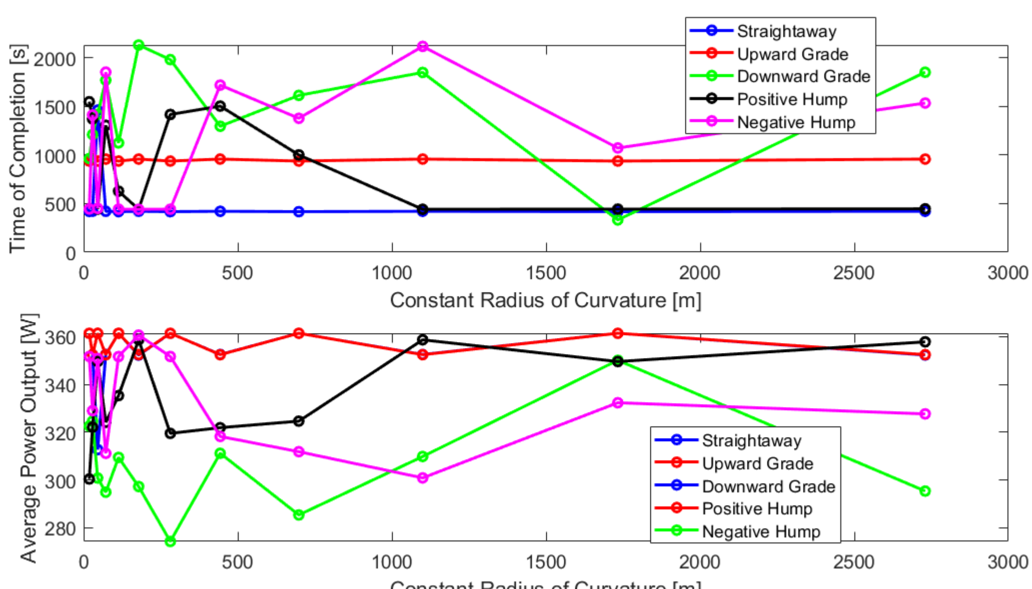

Figure 19: The time of convergence (upper subplot) and the average power outputted by the rider (lower subplot) for each of the course elements under the effects of an increasing constant radius of curvature. Rider parameter are chosen consistent with the male time trial specialist studied.

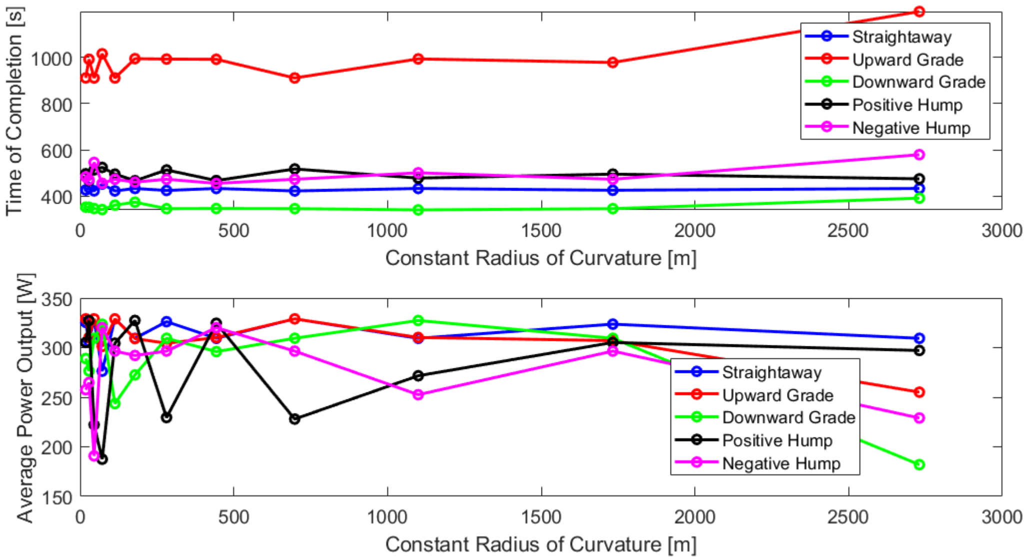

Figure 20: The time of convergence (upper subplot) and the average power outputted by the rider (lower subplot) for each of the course elements under the effects of an increasing constant radius of curvature. Rider parameters are chosen consistent with the male climber studied.

7.7 Extensions to General Tracks

To approximate the solution to a combination of course elements, it is important to consider the boundaries between concatenated course elements and the quantity of W' remaining at those boundaries. We define the boundary conditions for each of our course elements as the amount of W' expected to be used over the entirety of the element. The portion of an optimal solution over an individual element can then by calculated from our model by assigning the boundary condition as $W'_{capacity}$. The question then remains of how best to assign those boundary condition to get the most agreement between the concatenated solutions for individual elements and the solution for the entire course. We hypothesize that this partitioning of the total W' to obtain the boundary conditions will depend on the specific course elements used, as well as the maximum grade of each element. We define the maximum grade of each element to be the maximum deviation from $\phi = 0$ in the course element simulated. So for each of the examples shown in figures 13 through 17, the elements have a maximum grade of 5. By studying various examples of 2 or 3 course elements, each with normalized absolute grades of 5 degrees, we found good agreement between concatenating individual solutions and the solution to the full track, when $W'_{capacity}$ was partitioned evenly between the elements. For example, when concatenating elements 4 and 5 , the resulting power output is shown below in figure 21. Observe that this output is roughly a concatenation of the power outputs shown in figures 16 and 17.

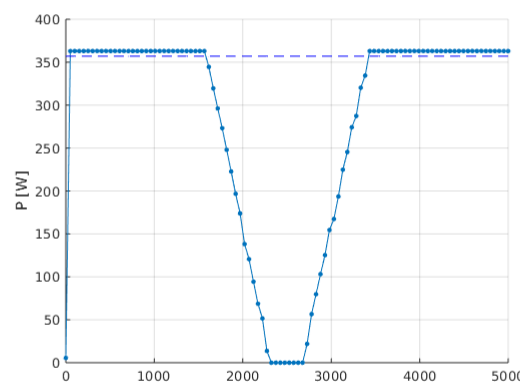

Figure 21: Power output over course consisting of concatenated elements 4 and 5. Rider parameters are chosen consistent with the female time trial specialist studied. The critical power for the rider is indicated with a dashed line.

More than two elements concatenated also generally display this behavior. For example, consider the concatenations of two elements 4s, element 1, and element 2, whose model generated optimal power output is shown below in figure 22. However, there is a change in amount of power output (from below critical power to above critical power) between the element 1 and 2 sections that would not be captured via the concatenation of power outputs alone.

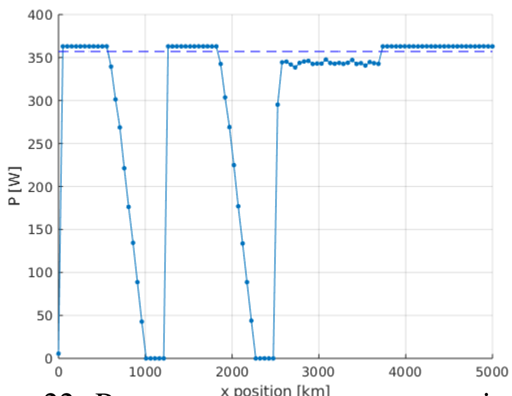

Figure 22: Power output over course consisting of concatenated elements 4, 4, 1 and 2. Rider parameters are chosen consistent with the female time trial specialist studied. The critical power for the rider is indicated with a dashed line.

7.8 Limitations and Benefits

The optimal solution to a series of course elements in general will not be the concatenation of optimal solutions to each of the elements and in many cases, the concatenation of element optimal solutions will necessarily be a sub-optimal solution for the whole course. For example, the most optimal way to traverse a straightaway will be different depending on whether or not it is followed by a upward grade because the rider should preserve W' in preparation to be used at the upward grade.
Imposing different boundary conditions on W' at the start and end of each element allows us to partially take these element-element interactions into account but not fully. A refinement of the optimal solution could be obtained by implementing more types of elements studied.

8 Other Extensions

8.1 Drafting

The model can be extended to take into account the interactions between rides via a varying C_d due to drafting. Drafting will generally changes the aerodynamic drag force acting on the ride and will be dependent on the configuration of the team. For a team of six riders, there may be 2 groups of 3 riders drafting, 3 groups of 2 riders drafting, 1 set of 6 riders in line draft or any such arrangement of less than 6 riders (if some riders are not drafting). The number of configurations greatly increases if we allow for non-in-line drafting (where the riders are not all perfectly in a line). These configurations could be discretely searched through using a method such as a Monte-Carlo tree search and for each, our model could be run to determine the optimal method and time for a certain rider in that configuration. Comparing the the times found for each configuration would allow us to determine the optimal solution and study optimal power distributions for each rider.
In a given configuration, a rider's C_d will be decreased depending on how many riders are in front of them and what kinds of riders they are (specifically the other rider's C_dA). Additionally, the maximum possible velocity that a rider can travel is limited by the rider ahead of them. To first order, we can determine the optimal pacing for the rider in the front with no variations to C_d, and then use the velocity found for the front rider as a constraint on the following riders.

9 Conclusion

By comparison to model results discussed in the literature [23–25, 28] we confirm the validity of the SQP numerical optimization scheme applied to the optimal control problem in certain regimes. We also confirm the validity of the extensions from [28] to include wind, track curvature and reconstitution of W'. The regimes in which we can conclude that our methods are valid are: 1) those in which there are only deviations in the course grade on large scales relative to the length of the course, 2) those where the weather conditions permit negligible changes in frictional coefficients and air density, and 3) those where the riders' bioenergetic parameters are within ranges expected for elite cyclists. Situations outside of these regimes may be possible with an alternative or improved numerical scheme.

We can approximate optimized behavior along complex tracks using the described course elements. Generally, solutions to concatenations of these elemental features resemble the concatenated solutions to individual elements under the correct boundary conditions. The ideal partitioning of W' across the discrete elements of the track to determine the boundary conditions is still an open question. We hypothesize that it will be dependent on the rider type, specific elements used to model the track, and the maximum grade of each element. In the model, perturbations due to wind act as stochastic perturbations in realistic track scenarios and affect the elements differently based on the standard deviation of wind conditions. At a certain level of σ_{wind} that may be applied, the downward grade decreases variability in time taken. The upward grade, straightaway, and negative hump greatly increase variability in times. The positive hump shows nearly no difference in variability in times. Using differences in this completion time as a metric of an optimal solutions deviation from the 0 headwind case, we can conclude that when using our model to determine differences in optimal strategy in light of uncertainty in wind, it will be important to know the wind variability threshold (for the case of the male time trial specialist discussed it is approximately 12 m/s) and the concentration of downward grades and positive humps. For courses with a lower concentration of those two elements, wind uncertainty beyond the threshold will result in a proposed power distribution to have a greater degree of deviation from the true optimal solution.

The curvature of the track has a different effect on the optimal solutions depending on the type of rider considered. It was determined that, when compared with the time trial specialist, the optimal time for climbers is less variable when perturbed by different constant radii of curvatures on our course elements, but their average power was equally variable. This is hypothesized to be due to the higher degree of variation in the climbers optimal power distribution over individual course elements, as well as their tendency to stay below CP. The average power and completion time for time trial specialists was less affected by wind for the upward grade and straightaway. Thus when using our model to plan an optimal power distribution for a time trial specialist, a higher concentration of straightaways and upward grades (as apposed to the other course elements) should inform a decrease in the consideration of track curvature. Similarly, track curvature should be considered less for a climber. In the case of a rider with parameters that necessitate more consideration of the curvature, the model of course elements could be extended to include elements determined by not only their grade, but also their curvature. For example, if we were to consider 5 curvature values we would have 5 different possible elements to partition our track into.

As expected, the time trial specialist's optimal strategy varied from the climber on the 3 full size courses studied. It was found that the ideal pacing for a time trial specialist is generally better performing than the idea pacing for the climber. Because the courses studied were all time trial-like, this is expected.

A rider's deviation from the precise, extreme changing in power output were found to be negligible in any cases studied. So, given that a rider's power trends will generally follow the same maxima and minima, the sharp changes or small variations in our model's optimal power distribution can be ignored.

Rider's Race Guidance for a Directeur Sportif

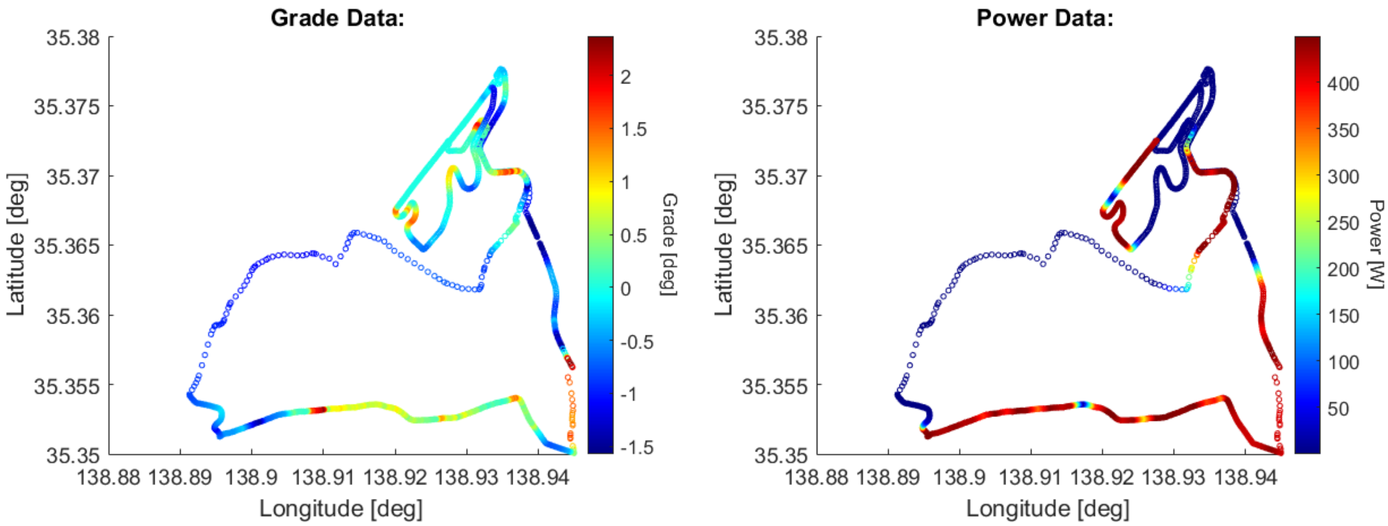

Figure 23: Optimal power output for the 2021 Tokyo Olympic Time Trial course for the time trial specialist with grade data from course (left) and power output (right) 24.

Improving track times on time trial courses at an elite level demands a sharp focus towards matching one's power output across the topography of a race to the strengths of their physiological profile. For riders focused on time trial cycling, the most important metric to consider is critical power (CP), which measures the maximum power output that can be sustained aerobically for a long time. Training towards increasing CP will result in an improved pace consistent across an entire course. CP is balanced by anaerobic work capacity (W') which measures the extra stored energy the body has to exert itself beyond one's CP. Compared to time trialists, riders specializing in climbing are more concerned with improving their W' as well as τ_w (recovery time) to overcome frequent steep inclines and recover quickly.

A mathematical model which inputs these characteristics of the rider in addition to the topology of a course provides rich information into the optimal strategy for how a rider should modulate their power output throughout a race. An output of this model for a male elite time trialist can be seen in Figure 23.

From model conclusions, the optimal strategy involves operating close to max power above one's CP during steep inclines, and dropping power down as much as possible during downhills to recover. On relatively straight sections, keeping pace at CP or just below it will minimize time without prompting exhaustion before the end of the race. This strategy can be seen clearly in Figure 24 plotting power against distance along the race.

For courses with more variation in grade, model outputs recommend operating more reactively to the course features. Alternatively, a flatter course prompts a pace which stays close to CP at all times. For any type of course, the goal is to deplete all excess energy W' by the time the finish line is reached. Clearly, elements of the course impact how one should distribute their excess energy; a course can be split into constituent elements to be used like basic building blocks which combined together give a reasonable approximation of a course. Five elements based on topography are defined, the model outputs for these are seen in Figure 25. On straightaways and upward grades, the same ideal strategy applies: output consistent power close to or above CP. On downward grades there is an opportunity to restore W' by decreasing power output, and this can also be seen on the downhill portion of the positive and negative hump. For time trialists, the optimal strategy when going over a hump is to go all-out up the hill, taper off, and recover as much as possible downhill. The inverse roughly applies to the negative hump.

Breaking up a course into its elements in preparation for a race and training on those elements both individually and combined is an excellent way train for a specific course. Worth noting is that the order of course elements further informs pacing: several steep inclines at the end of an otherwise flat race for example will change a strategy to save more W' than normal for powering up grades at the end of the race. In that case, operating only below CP on straightaways would be optimal.

Due consideration should be taken into the environmental 'perturbations' of the course, chiefly a strong headwind and the locations of sharp turns. If a headwind is greater than 15m/s, model outputs indicate that changing power output reactively to the wind rather than staying consistent will lower track times. For sharp turns, more concern should be given towards turns on steep grades. For longer courses, sharp turns are less impactful overall. Training in an environment similar to one expected on race day will be the most informative towards improvement, particularly for courses at elevation which will diminish a rider's $V_{02_{max}}$.

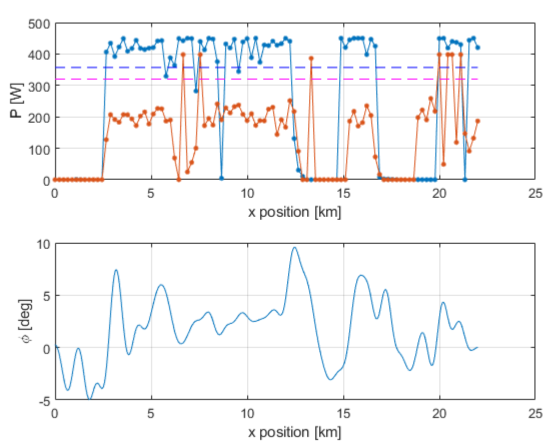

Figure 24: Optimal power output (upper subplot) corresponding to ϕ (grade) values from Tokyo Time Trial shown in lower subplot. Male time trial parameters were used for the power output shown in blue, with CP noted by the dark blue dotted line. Climber output shown for comparison.

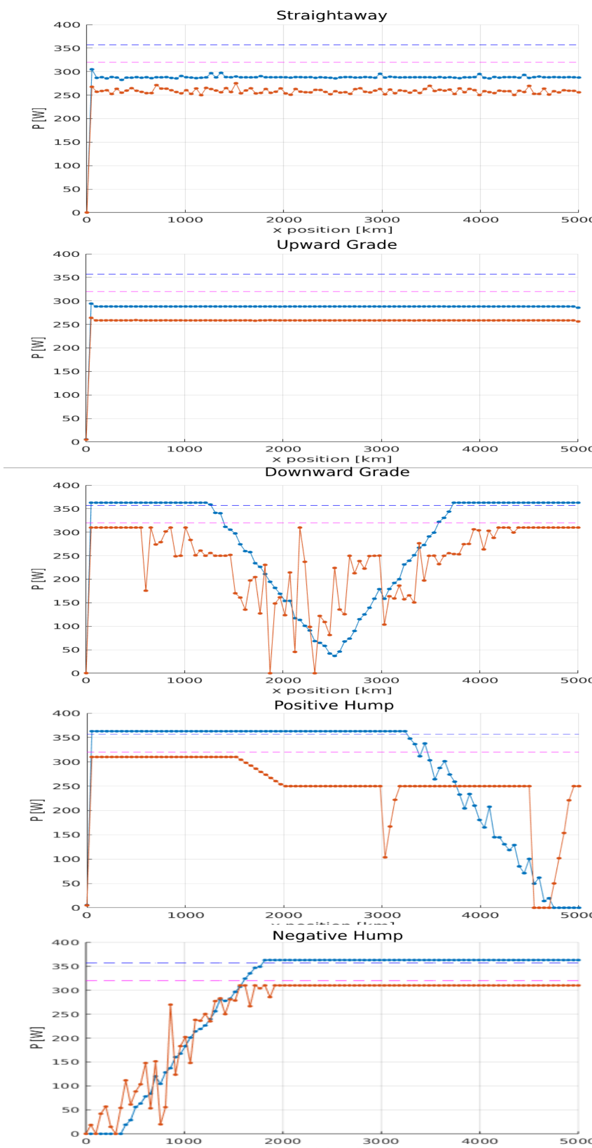

Figure 25: Model generated optimal power output along all five course elements. CP was set lower than Tokyo, and denoted by the dark blue dotted line. Climber output shown for comparison.

References

[1] H. Monod, J. Scherrer, *Ergonomics* **1965**, *8*, 329–338.

[2] M. R. Oxford, *Physical Therapy* **1978**, *58*, 1018–1020.

[3] H. A. deVries, M. W. Tichy, T. J. Housh, K. D. Smyth, A. M. Tichy, D. J. Housh, *Ergonomics* **1987**, *30*, 1195–1204.

[4] D. C. Poole, S. A. Ward, G. W. Gardner, B. J. Whipp, *Ergonomics* **1988**, *31*, 1265–1279.

[5] T. J. Housh, G. O. Johnson, S. L. McDowell, D. J. Housh, M. Pepper, *Int J Sports Med* **1991**, *12*, 305–308.

[6] D. W. Hill, *Sports Medicine* **1993**, *16*, 237–254.

[7] A. Barclay, P. E. Gill, J. Ben Rosen in Variational Calculus, Optimal Control and Applications, (Eds.: W. H. Schmidt, K. Heier, L. Bittner, R. Bulirsch), Birkhäuser Basel, Basel, **1998**, pp. 207–222.

[8] J. J. de Koning, M. F. Bobbert, C. Foster, *Journal of Science and Medicine in Sport* **1999**, *2*, 266–277.

[9] S. Padilla, I. Mujika, G. Cuesta, J. J. Goiriena, *Medicine and science in sports and exercise* **1999**, *31 6*, 878–85.

[10] K. L. Teo, L. S. Jennings, H. W. J. Lee, V. Rehbock, *The Journal of the Australian Mathematical Society. Series B. Applied Mathematics* **1999**, *40*, 314–335.

[11] V. L. Billat, *British Journal of Sports Medicine* **2000**, *34*, 83–85.

[12] I. Mujika, S. Padilla, *Sports Med* **2001**, *31*, 479–487.

[13] S. Gordon, *Sports Engineering* **2005**, *8*, 81–90.

[14] R. Morton, *European journal of applied physiology* **2006**, *96*, 339–54.

[15] G. Atkinson, O. Peacock, L. Passfield, *Journal of Sports Sciences* **2007**, *25*, PMID: 17497402, 1001–1009.

[16] F. Impellizzeri, T. Ebert, A. Sassi, P. Menaspà, E. Rampinini, D. Martin, *European journal of applied physiology* **2008**, *102*, 335–41.

[17] A. M. Jones, D. P. Wilkerson, F. DiMenna, J. Fulford, D. C. Poole, *American Journal of Physiology-Regulatory Integrative and Comparative Physiology* **2008**, *294*, PMID: 18056980, R585–R593.

[18] C. Ferguson, H. B. Rossiter, B. J. Whipp, A. J. Cathcart, S. R. Murgatroyd, S. A. Ward, *Journal of Applied Physiology* **2010**, *108*, PMID: 20093659, 866–874.

[19] P. Cangley, L. Passfield, H. Carter, M. Bailey, *Int J Sports Med* **2011**, *32*, 132–136.

[20] A. Nimmerichter, R. Eston, Bachl, C. Williams in **2011**.

[21] P. Skiba, W. Chidnok, A. Vanhatalo, A. Jones, *Medicine and science in sports and exercise* **2012**, *44*, 1526–32.

[22] H. Badreddine, S. Vandewalle, J. Meyers, *Journal of Computational Physics* **2014**, *256*, 1–16.

[23] D. Sundström, P. Carlsson, M. Tinnsten, *Sports Engineering* **2014**, *17*, 207–215.

[24] L. Underwood, M. Jermy, *Sports Engineering* **2014**, *17*, 183–196.

[25] J. de Jong, R. Fokkink, G. J. Olsder, A. Schwab, *Procedia Engineering* **2016**, *147*, The Engineering of SPORT 11, 907–911.

[26] M. S. Wells, S. Marwood, *Eur J Sport Sci* **2016**, *16*, 912–918.

[27] A. Bossi, C. O'Grady, R. Ebreo, L. Passfield, J. Hopker, *International Journal of Sports Physiology and Performance* **2017**, *13*, 1–23.

[28] J. Jong, R. Fokkink, G. Olsder, A. Schwab, *Proceedings of the Institution of Mechanical Engineers Part P: Journal of Sports Engineering and Technology* **2017**, *231*, 175433711770505.

[29] J. C. Bartram, D. Thewlis, D. T. Martin, K. I. Norton, *International journal of sports physiology and performance* **2018**, *13 6*, 724–728.

[30] P. T. Morgan, M. I. Black, S. J. Bailey, A. M. Jones, A. Vanhatalo, *J Sports Sci* **2019**, *37*, 902–910.

[31] S. Wolf, PhD thesis, Universität Konstanz, Konstanz, **2019**.

[32] K. Phillips, W. Hopkins, *Sports Medicine - Open* **2020**, DOI `10.1186/s40798-020-00252-z`.

[33] P. Leo, J. Spragg, T. Podlogar, J. S. Lawley, I. Mujika, *European Journal of Applied Physiology* **2022**, *122*, 301–316.